Available online at www.sciencedirect.com
SCIENCE DIRECT®
Bioorganic & Medicinal Chemistry Letters 15 (2005) 5247–5252
Bioorganic & Medicinal Chemistry Letters

# Synthesis, biological activity, and X-ray crystal structural analysis of diaryl ether inhibitors of malarial enoyl acyl carrier protein reductase. Part 1: 4′-Substituted triclosan derivatives

Joel S. Freundlich,[a,*] John W. Anderson,[a] Dimitri Sarantakis,[a] Hong-Ming Shieh,[a] Min Yu,[b] Juan-Carlos Valderramos,[b] Edinson Lucumi,[d] Mack Kuo,[d] William R. Jacobs, Jr.[b,c] David A. Fidock,[b] Guy A. Schiehser,[a] David P. Jacobus[a] and James C. Sacchettini[d]

[a]*Department of Medicinal Chemistry, Jacobus Pharmaceutical Company, 37 Cleveland Lane, Princeton, NJ 08540, USA*
[b]*Department of Microbiology and Immunology, Albert Einstein College of Medicine, Bronx, NY 10461, USA*
[c]*Howard Hughes Medical Institute, Albert Einstein College of Medicine, Bronx, NY 10461, USA*
[d]*Department of Biochemistry and Biophysics, Texas A&M University, College Station, TX 77843-2128, USA*

Received 1 June 2005; revised 9 August 2005; accepted 17 August 2005
Available online 29 September 2005

**Abstract**—A structure-based approach has been taken to develop 4′-substituted analogs of triclosan that target the key malarial enzyme *Plasmodium falciparum* enoyl acyl carrier protein reductase (PfENR). Many of these compounds exhibit nanomolar potency against purified PfENR enzyme and modest (2–10 μM) potency against in vitro cultures of drug-resistant and drug-sensitive strains of the *P. falciparum* parasite. X-ray crystal structures of nitro **29**, aniline **30**, methylamide **37**, and urea **46** demonstrate the presence of hydrogen-bonding interactions with residues in the active site and point to future rounds of optimization to improve compound potency against purified enzyme and intracellular parasites.


The development of novel anti-malarials is critical as malaria worldwide afflicts 300–600 million people resulting in 1–3 million deaths per year.[1,2] *Plasmodium falciparum* infection is the most widespread form of malaria and is the predominant cause of severe disease and death. Traditional treatments with drugs, such as chloroquine and sulfadoxine-pyrimethamine, are now much less effective due to rampant resistance.[3]

The inhibition of fatty acid synthesis in *P. falciparum* holds significant promise in potentially enabling the discovery and development of an orally dosed therapeutic that is affordable, safe, and efficacious against drug-resistant strains. Fatty acid synthesis plays a key role in membrane construction and energy production. Unlike in higher eukaryotes and yeast where fatty acid biosynthetic machinery resides on a single multifunctional polypeptide (FAS-I), fatty acid synthesis in *Plasmodium* is reliant on a dissociative process that utilizes a set of distinct enzymes composing a FAS-II pathway.[4] This pathway has been localized to the parasite apicoplast, an essential organelle ancestrally related to cyanobacteria.[5] Fatty acid biosynthesis is an iterative process beginning with the condensation of acetyl CoA with the growing fatty acid chain. *P. falciparum* enoyl acyl carrier protein (ACP) reductase (PfENR) is responsible for the final step in each fatty acid synthesis cycle: the NADH-dependent reduction of *trans*-2-enoyl-ACP to acyl-ACP.

We and others have shown that triclosan inhibits PfENR,[6,7] in addition to the related ENRs for *Escherichia coli*,[8,9] *Staphylococcus aureus*,[10] and mycobacteria.[11] This compound was also found to be effective in killing *P. falciparum* in vitro[6,7,12] and curing mice of infection with the rodent malaria species *Plasmodium berghei*.[6] Given triclosan's abundance[13] (U.S. annual production $> 1 \times 10^6$ lbs), its safety as demonstrated by its widespread use in personal care and household products, and the absence of a lipid synthesis inhibitor in the anti-malarial arsenal, we and others have chosen to

*Keywords*: Anti-malarial; Phenol; Diaryl ether.
* Corresponding author. Tel.: +1 609 9217447; fax: +1 609 7991176; e-mail: j_freundlich@jacobuspharm.com

0960-894X/$ - see front matter © 2005 Elsevier Ltd. All rights reserved.
doi:10.1016/j.bmcl.2005.08.044

pursue the discovery of a triclosan-derived therapeutic for malaria.[7,14–19]

Prior elucidation of the X-ray crystal structure of triclosan and its $NAD^+$ co-factor bound to PfENR revealed the phenol moiety to be the critical binding element of triclosan.[7] Structural analysis suggested vectors off the triclosan A and B rings where additional functionality could be placed to enhance binding affinity. A strategy was developed to build off these aromatic ring positions to enhance enzymatic and anti-parasitic activity. A significant gain in potency could facilitate replacement or removal of the phenol, which is a metabolic liability as in vivo conjugation of the phenol leads to rapid clearance of triclosan.[20] With this goal in mind, this report details our work on the 4′-position of the triclosan pharmacophore.

Examination of the PfENR:$NAD^+$:triclosan structure revealed the 4′-chloro group to be in van der Waals contact with the hydrophobic sidechains of Val-222 and Met-281. The halogen is directed toward the sidechain of Asn-218 and backbone carbonyl of Ala-219. Our hypothesis was that replacement of the chloride with a variety of groups with both hydrophobic and hydrogen-bonding characteristics could enhance the enzyme binding affinity of triclosan derivatives. A recently reported triclosan analog utilizes the hydroxyl group of a naphthol to make these proposed hydrogen bonds.[7] The 4′-chloro is approximately 4 Å from the solvent-accessible surface and, thus, the 4′-position could also serve to append functionality to alter inhibitor physiochemical properties.

Compound syntheses began with nitroaromatic **1**, aldehyde **2**, and nitrile **3**, prepared from commercially available starting materials via nucleophilic aromatic substitution. Elaboration of the nitro derivative **1** is depicted in Scheme 1. Compound **1** was hydrogenated to afford aniline **4** which could be acylated or sulfonylated to afford **5**–**10**. Reductive amination with aldehydes

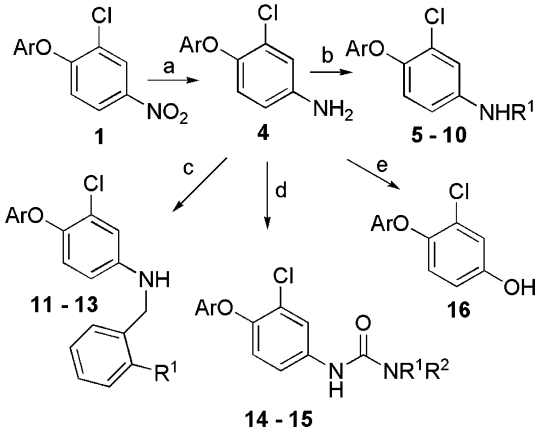


**Scheme 1.** Synthesis of various 4′-derivatives from the corresponding parent aniline where Ar = 4-chloro-2-methoxyphenyl. Reagents and conditions: (a) $H_2$, Ra-Ni, AcOH/EtOH, (b) $Ac_2O$ or PhC(O)Cl or $RSO_2Cl$ in $NEt_3$, DCM; (c) ArCHO, $NaBH_3CN$, HOAc, MeOH; (d) i—$(Cl_3CO)_2CO$, $NEt_3$, DCM, −78 °C rt, ii—$R^1R^2NH$; (e) i—$H_2SO_4$, $NaNO_2$, 0 °C, ii—tol, 110 °C.

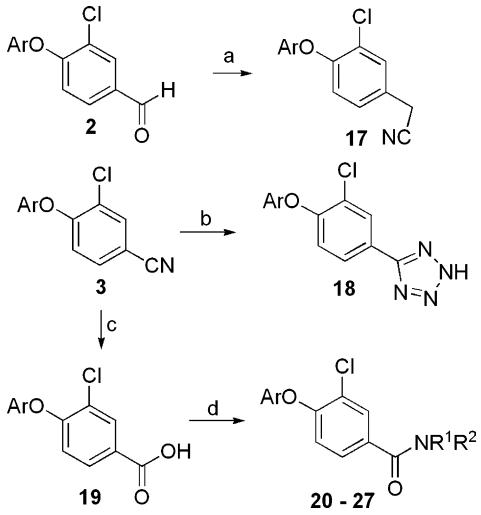


**Scheme 2.** Synthesis of various 4′-derivatives from the corresponding aldehyde and nitrile derivatives, where Ar = 4-chloro-2-methoxyphenyl. Reagents: (a) i—$LiAlH_4$, THF, ii—TsCl, $NEt_3$, DCM, iii—NaCN, DMSO; (b) $NaN_3$, $ZnBr_2$, $H_2O$, Δ; (c) NaOH, $H_2O_2$, THF, 70–90 °C; (d) i—HBTU, $HNR^1R^2$, DIEA, DMF/NMP or ii—cat. DMF, $SOCl_2$ then $HNR^1R^2$.

yielded **11**–**13**. Activation of the aniline with triphosgene in the presence of base followed by aminolysis afforded ureas **14**–**15**. Diazotization of the aniline followed by acid hydrolysis of the corresponding diazonium salt afforded 4′-phenol **16**.[21]

As shown in Scheme 2, aldehyde **2** was reacted in three steps to produce **17** via a sequence of conventional methods consisting of lithium aluminum hydride reduction, tosylation, and displacement with sodium cyanide. The method of Sharpless was implemented to prepare tetrazole **18** from nitrile **3**.[22] Sodium hydroperoxide was generated in situ and utilized to hydrolyze **3** to carboxylic acid **19**.[23] The carboxylic acid was taken on to afford amides **20**–**27** using either acid chloride methodology or HBTU-mediated coupling.

The intermediate anisoles **1** and **3**–**27** were treated with an excess of boron tribromide or aluminum trichloride to derive the final product phenols **28**–**53**. All final compounds were characterized by $^1H$ NMR, LC–MS, and in some cases elemental analysis.

Final compounds **28**–**53** were tested in two assay systems to determine their inhibition of PfENR enzymatic activity and inhibition of parasite whole cell growth. For both assays, the reported inhibitory concentrations are tabulated as means ± standard error, taking into account three independent determinations performed in duplicate. The enzyme assay has been previously described[7] and was modified slightly to allow for a higher throughput.[25] Briefly, the assay measured the NADH-dependent enzymatic reduction of crotonoyl-CoA substrate by following a decrease in absorbance at 340 nm resulting from the conversion of NADH to $NAD^+$. To date, 14 independent determinations of the $IC_{50}$ of triclosan have been made, resulting in a mean of 73 nM with a standard error of 21 nM. The parasite whole cell

assay, previously described,[7] uses [$^3$H]hypoxanthine incorporation into nucleic acids in cultured *P. falciparum* parasites (exposed to drug for 72 h) as a marker of growth inhibition in the presence of drug. In the current study, two parasite strains were utilized: 3D7, which is drug-sensitive, and Dd2, which is resistant to the antimalarials chloroquine and pyrimethamine-sulfadoxine.[24] To date, 43 independent runs of triclosan have been conducted with the following results. Against the 3D7 strain, the $EC_{50}$ was determined to have a mean value of 2.9 μM and a standard error of 0.2 μM. Versus the Dd2 strain, the $EC_{50}$ mean value was 3.9 μM with a standard error of 0.3 μM.

Table 1 shows the results from biological testing of the initial round of compounds (**28**–**36**), which targeted replacement of the 4′-chloro group with simple organic functionality capable of hydrogen bonding with Asn-218 and Ala-219. All compounds in this subset display $IC_{50}$ values <400 nM, except for molecules featuring a relatively acidic proton: carboxylic acid **33**, tetrazole **34**, and hydroxamic acid **36**. Sharing the common feature of a hydrogen bond acceptor, amide **35** and nitrile **31** are among the most potent of these derivatives against the enzyme. Consistent with its enzymatic activity, **31** exhibits parasite activity equipotent to triclosan. **35**, however, suffers a significant loss against the parasite, while nitro derivative **29** exhibits potent anti-parasite activity. The significant anti-parasitic efficacy of **29** is not commensurate with its enzyme inhibition and off-target activity must be considered as an explanation.

Utilizing the criteria of enzymatic potency and ease of synthetic elaboration, the amide **35** core was chosen for analog synthesis with the dual goals of improving enzyme and parasite assay potency. Aniline **30**, although less potent than **35** in both assay systems, was also selected for derivatization due to the facile nature of the synthetic chemistry. Not only could an increase in compound hydrophobicity potentially aid parasite membrane permeability, but the potential of interacting with other hydrophobic moieties (i.e., Val-222, Tyr-277, and Met-281) within the PfENR active site held promise.

Inspection of the biological data in Table 2 for amide derivatives **35**, **37**–**42** does not afford a clear SAR trend. With regard to enzyme inhibition, the parent amide **35** is most potent, with the morpholino amide **42** being most preferable amongst the tertiary amides tested. This trend is not reflected in the parasite assay, where the benzylamide **38** and piperidino amide **41** are the most

**Table 1.** Inhibitory properties of selected 4′-substituted derivatives.

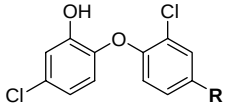


| Compound | R | $EC_{50}$[a] 3D7/Dd2 (μM) | PfENR[a] $IC_{50}$ (nM) |
|---|---|---|---|
| Triclosan | Cl | 2.9 ± 0.2/3.9 ± 0.3 | 73 ± 21 |
| **28** | OH | 65.3 ± 9.2/87.8 ± 20.6 | 220 ± 25 |
| **29** | $NO_2$ | 2.1 ± 0.1/3.2 ± 0.6 | 180 ± 22 |
| **30** | $NH_2$ | 120 ± 21/140 ± 24 | 360 ± 92 |
| **31** | CN | 3.9 ± 0.7/5.4 ± 0.7 | 120 ± 43 |
| **32** | $CH_2CN$ | 23.1 ± 5.1/36.4 ± 3.7 | 190 ± 52 |
| **33** | COOH | 110 ± 27/130 ± 4 | 550 ± 20 |
| **34** | 1H-tetrazol-5-yl | 120 ± 10/>150 | 413 ± 49 |
| **35** | $C(O)NH_2$ | 96.3 ± 11.7/100 ± 16 | 120 ± 35 |
| **36** | C(O)NHOH | 31.2 ± 10.8/30.6 ± 2.2 | 1200 ± 240 |

[a] Values reported as means ± standard error.

**Table 2.** Inhibitory properties of selected 4′-amide derivatives.

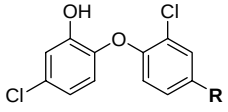


| Compound | R | $EC_{50}$[a] 3D7/Dd2 (μM) | PfENR[a] $IC_{50}$ (nM) |
|---|---|---|---|
| **35** | $NH_2$ | 96.3 ± 11.7/100 ± 16 | 120 ± 35 |
| **37** | N(H)Me | 77.8 ± 25.3/100 ± 22 | 310 ± 66 |
| **38** | N(H)Bn | 7.5 ± 2.8/20.6 ± 3.6 | 3000 ± 800 |
| **39** | $NMe_2$ | 68.4 ± 13.2/95.7 ± 11.6 | 460 ± 110 |
| **40** | *N*-Pyrrolidine | 20.7 ± 6.0/42.6 ± 12.8 | 810 ± 300 |
| **41** | *N*-Piperidine | 11.7 ± 2.2/18.0 ± 3.0 | 680 ± 120 |
| **42** | *N*-Morpholine | 63.5 ± 14.1/94.5 ± 10.0 | 200 ± 10 |

[a] Values reported as means ± standard error.

efficacious. Clearly, gains in anti-parasitic activity can be made by substituting for one or more of the parent amide's N–H groups. Further rounds of compound synthesis and assay evaluation are necessary to clarify the structural requirements for attaining both enzyme and parasite assay activity. It is interesting to note that the substituted amides **37**–**42** are significantly more potent against the 3D7 strain than the Dd2 strain.

The assay data for aniline derivatives **43**–**53** are shown in Table 3. Acyl-based derivatives such as the acetyl **43** and benzoyl **44** analogs display modest improvements in both assay systems. The sulfonamide analog of **44** is equipotent against cultured parasites, while being less active against purified enzyme. Alteration of the sulfonamide aryl group from phenyl (**47**) to 1- or 2-naphthyl (**48** and **49**) offers slight improvements in parasite assay performance while resulting in decreased enzyme inhibition.

Benzylamine derivative **51** exhibits greater potency than aniline **30** against purified enzyme and cultured parasites. Introduction of an *ortho*-substituent in **52** and **53** affords more potent compounds than **51** in the parasite assay, while not improving enzyme inhibition. *Ortho*-phenol **53** is much more potent against the parasite ($EC_{50}$ = 4.5 (3D7) and 5.6 (Dd2) μM) than **30**, while not exhibiting enhanced enzyme inhibition.

To understand the molecular basis of these results, we have solved the X-ray crystal structures of nitro **29**, aniline **30**, methylamide **37**, and urea **46** bound to PfENR in the presence of co-factor. As expected, the only significant difference in all of these structures is the interaction of the 4′-substituent with the surrounding enzyme residues. Other interactions of the triclosan core with co-factor and enzyme are preserved. Displayed in Figure 1, **30** utilizes its aniline hydrogens to form hydrogen bonds to the side-chain carbonyl of Asn-218 ($d_{C=O-N}$ = 3.4 Å) and the main chain carbonyl of Ala-219 ($d_{C=O-N}$ = 3.7 Å). The aniline nitrogen's lone pair may be engaged in a favorable interaction with the main chain N–H group of Ala-219 ($d_{N-N}$ = 2.7 Å). Compound **29** binds in a conformation similar to **30**. The only significant change in the enzyme active site is the rotation of the Asn-218 sidechain to allow its carboxamide N–H to interact with one of the nitro oxygens ($d_{N-O}$ = 3.4 Å). The same nitro oxygen forms a hydrogen bond with the main chain N–H group of Ala-219 ($d_{N-O}$ = 3.2 Å), while the other oxygen makes no direct interactions with the enzyme.

Methylamide derivative **37**, shown in Figure 2, utilizes its amide carbonyl to form a hydrogen bond with the sidechain N–H of Asn-218 ($d_{N-O=C}$ = 3.2 Å) and the carbonyl may also make a weak hydrogen bond with

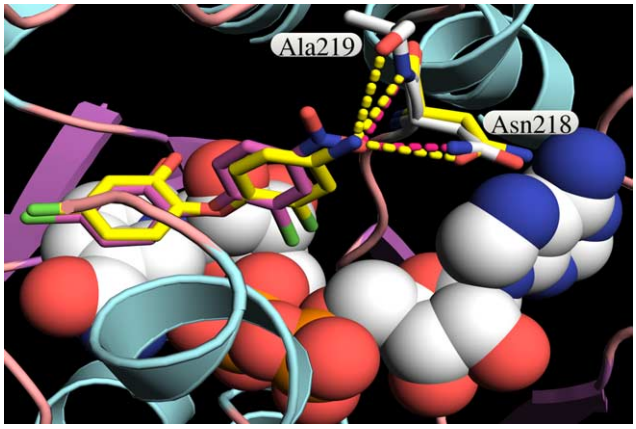


**Figure 1.** Overlay of the X-ray structures of **29** (stick drawing with carbons in yellow) and **30** (stick drawing with carbons in purple) in the PfENR active site (ribbon and tube with key residues in stick format) with bound co-factor (space-fill). One of the nitro oxygens of **29** is hydrogen-bonded to the side-chain amide N–H of Asn-218 and the backbone N–H of Ala-219. The 4′-anilino hydrogens of **30** are hydrogen-bonded to the side-chain carbonyl of Asn-218 and the main chain carbonyl of Ala-219. The aniline lone pair may be participating in a hydrogen bond with the main chain N–H of Ala-219.

**Table 3.** Inhibitory properties of selected 4′-aniline derivatives.

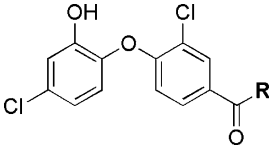


| Compound | R | $EC_{50}$[a] 3D7/Dd2 (μM) | PfENR[a] $IC_{50}$ (nM) |
|---|---|---|---|
| **30** | H | 120 ± 21/140 ± 24 | 360 ± 92 |
| **43** | Ac | 52.2 ± 17.3/50.9 ± 19.2 | 57 ± 24 |
| **44** | Bz | 57.2 ± 14.7/83.9 ± 15.0 | 170 ± 16 |
| **45** | $C(O)NH_2$ | 110 ± 24/120 ± 22 | 160 ± 45 |
| **46** | C(O)*N*-Morpholine | 66.8 ± 14.1/86.4 ± 14.9 | 250 ± 49 |
| **47** | $SO_2Ph$ | 55.1 ± 10.2/77.5 ± 8.0 | 370 ± 100 |
| **48** | $SO_2$(1-Naphthyl) | 34.3 ± 5.6/43.7 ± 12.2 | 590 ± 88 |
| **49** | $SO_2$(2-Naphthyl) | 23.5 ± 3.2/33.9 ± 9.6 | 2500 ± 900 |
| **50** | $SO_2CF_3$ | >120/>120 | 140 ± 34 |
| **51** | $CH_2Ph$ | 35.8 ± 5.3/47.5 ± 12.2 | 140 ± 69 |
| **52** | $CH_2$(2-CNPh) | 26.7 ± 2.9/45.4 ± 6.5 | 560 ± 120 |
| **53** | $CH_2$(2-HOPh) | 4.5 ± 0.5/5.6 ± 1.3 | 320 ± 59 |

[a] Values reported as means ± standard error.

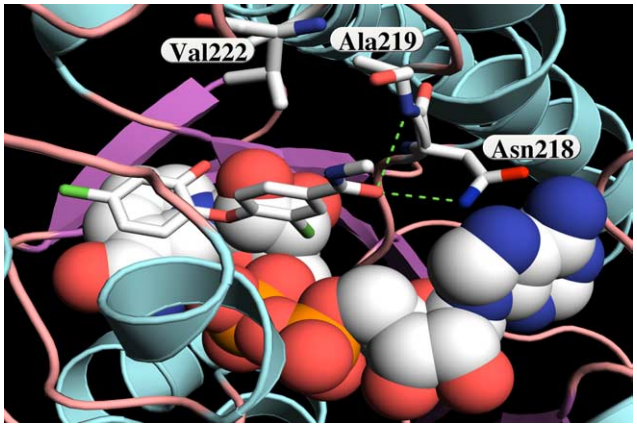


**Figure 2.** X-ray structure of **37** (stick drawing) in the PfENR active site (ribbon and tube with key residues in stick format) with bound co-factor (space-fill). The 4′-methylamide carbonyl group makes a hydrogen bond with the side-chain N–H of Asn-218 and it may also be engaged in a weak hydrogen bond with the backbone N–H of Ala-219. The amide methyl group is interacting with the Val-222 sidechain.

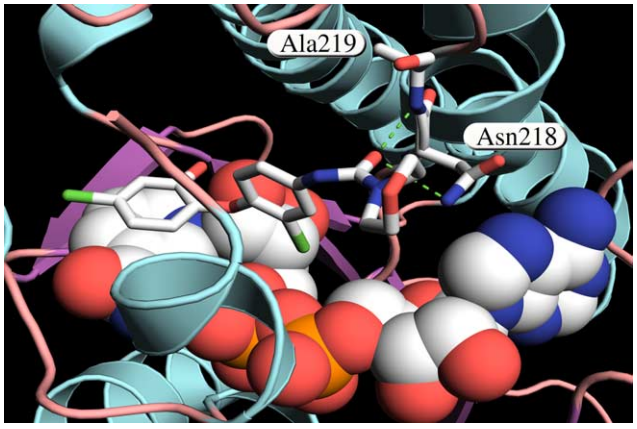


**Figure 3.** X-ray structure of **46** (stick drawing) in the PfENR active site (ribbon and tube with key residues in stick format) with bound co-factor (space-fill). The 4′-urea carbonyl group is hydrogen bonded with the sidechain N–H of Asn-218 and the backbone N–H of Ala-219.

the main chain N–H group of Ala-219 ($d_{N-O=C}$ = 4.0 Å). Its *N*-methyl group appears to interact favorably with the *i*-propyl sidechain of Val-222. Depicted in Figure 3, the urea derivative **46**, in contrast, does not have significant interactions between the appended morpholino group and the enzyme. The urea carbonyl moiety is hydrogen bonded to the Asn-218 sidechain N–H group ($d_{N-O=C}$ = 2.8 Å) and the Ala-219 main chain N–H ($d_{N-O=C}$ = 3.0 Å).

Clearly, the crystal structures of **29**, **30**, **37**, and **46** demonstrate the ability to append hydrogen-bonding functionality off the 4′-position through interactions with Asn-218 and Ala-219. However, from the enzyme data in Tables 1–3, it is clear that overall losses in binding affinity for the enzyme are realized. The reasons for these decreases in enzyme binding are not clear at this moment. One can speculate that, in the structurally characterized analogs, replacement of the chloro with a more polar group such as anilino, nitro, carboxamido, or ureido may result in the loss of hydrophobic interactions with Val-222 and Met-281. Subtle rearrangements in the enzyme complex with co-factor and ligand may also be responsible for the observed decreases in ligand affinity.

In conclusion, a series of 4′-substituted triclosan derivatives have been prepared and assayed for inhibition of purified PfENR and cultured *P. falciparum*. While the effort did not result in compounds significantly more potent than triclosan against both the enzyme and the parasite, it did provide an understanding of which groups could be substituted for the 4′-chloro to provide nanomolar inhibitors of PfENR with demonstrated anti-parasitic activity. X-ray crystallography studies demonstrate the ability of some of the prepared compounds to expand upon triclosan's interactions with PfENR via hydrogen-bonding networks with Asn-218 and Ala-219. The examination of the 4′-position will aid future efforts guided toward improving the potency and pharmacokinetic profiles of this diaryl ether class of anti-malarials. This will be done in conjunction with probing other positions along the diaryl ether scaffold.

## Acknowledgment

This work has been supported by funding from the Medicines for Malaria Venture.

## Supplementary data

Supplementary data associated with this article can be found in the online version, at doi:10.1016/j.bmcl.2005.08.044

## References and notes

1. Fidock, D. A.; Rosenthal, P. J.; Croft, S. L.; Brun, R.; Nwaka, S. *Nat. Rev. Drug Discov.* **2004**, *3*, 509.
2. Snow, R. W.; Guerra, C. A.; Noor, A. M.; Myint, H. Y.; Hay, S. I. *Nature* **2005**, *434*, 214.
3. Greenwood, B.; Mutabingwa, T. *Nature* **2002**, *415*, 670.
4. Schweizer, E.; Hofmann, J. *Microbiol. Mol. Biol. Rev.* **2004**, *68*, 501.
5. Ralph, S. A.; van Dooren, G. G.; Waller, R. F.; Crawford, M. J.; Fraunholz, M. J.; Foth, B. J.; Tonkin, C. J.; Roos, D. S.; McFadden, G. I. *Nat. Rev. Microbiol.* **2004**, *2*, 203.
6. McLeod, R.; Muench, S. P.; Rafferty, J. B.; Kyle, D. E.; Mui, E. J.; Kirisits, M. J.; Mack, D. G.; Roberts, C. W.; Samuel, B. U.; Lyons, R. E.; Dorris, M.; Milhous, W. K.; Rice, D. W. *Int. J. Parasitol.* **2001**, *31*, 109.
7. Perozzo, R.; Kuo, M.; bir Singh Sidhu, A.; Valiyaveettil, J. T.; Bittman, R.; Jacobs, W. R., Jr.; Fidock, D. A.; Sacchettini, J. C. *J. Biol. Chem.* **2002**, *277*, 13106.
8. McMurry, L.; Oethinger, M.; Levy, S. B. *Nature* **1998**, *394*, 531.
9. Heath, R. J.; Rubin, J. R.; Holland, D. R.; Zhang, E.; Snow, M. E.; Rock, C. O. *J. Biol. Chem.* **1999**, *274*, 11110.
10. Heath, R. J.; Li, J.; Roland, G. E.; Rock, C. O. *J. Biol. Chem.* **2000**, *275*, 4654.

11. McMurry, L.; McDermott, P. F.; Levy, S. B. *Antimicrob. Agents Chemother.* **1999**, *43*, 711.
12. Surolia, N.; Surolia, A. *Nat. Med.* **2001**, *7*, 167.
13. www.scorecard.com/chemical~profiles.
14. Kapoor, M.; Gopalakrishnapai, J.; Surolia, N.; Surolia, A. *Biochem. J.* **2004**, *381*, 735.
15. Kapoor, M.; Mukhi, P. L. S.; Surolia, N.; Suguna, K.; Surolia, A. *Biochem. J.* **2004**, *381*, 725.
16. Kapoor, M.; Reddy, C. C.; Krishnasastry, M. V.; Surolia, N.; Surolia, A. *Biochem. J.* **2004**, *381*, 719.
17. Kuo, M. R.; Morbidoni, H. R.; Alland, D.; Sneddon, S. F.; Gourlie, B. B.; Staveski, M. M.; Leonard, M.; Gregory, J. S.; Janjigian, A. D.; Yee, C.; Musser, J. M.; Kreiswirth, B.; Iwamoto, H.; Perozzo, R.; Jacobs, W. R., Jr.; Sacchettini, J. C.; Fidock, D. A. *J. Biol. Chem.* **2003**, *278*, 20851.
18. Rao, S. P. R.; Surolia, A.; Surolia, N. *Mol. Cell. Biochem.* **2003**, *253*, 55.
19. Surolia, N.; RamachandraRao, S. P.; Surolia, A. *BioEssays* **2002**, *24*, 192.
20. Wang, L.-Q.; Falany, C. N.; James, M. O. *Drug. Metab. Dispos.* **2004**, *32*, 1162.
21. Wataya, M.; Onodera, N.; Imamura, S. U.S. Patent 4,005,151, 1977.
22. Demko, Z. P.; Sharpless, K. B. *J. Org. Chem.* **2001**, *66*, 7945.
23. Davis, F. A.; Reddy, G. V.; Chen, B.-C.; Kumar, A.; Haque, M. S. *J. Org. Chem.* **1995**, *60*, 6148.
24. Wellems, T. E.; Panton, L. J.; Gluzman, I. Y.; de Rosario, V. E.; Gwadz, R. W.; Walker-Jonah, A.; Krogstad, D. J. *Nature* **1990**, *345*, 253.
25. Experiments were carried out on a BMG LABTECH FLUOstar OPTIMA multifunctional microplate reader at 25 °C in 20 mM Tris, pH 8.0, 150 mM NaCl, 10 mM EDTA, and 1 mM DTT at a total volume of 200 μL using 50 nM PfENR 400 μM NADH and 40 μM $NAD^+$ The reactions were initiated with $C_4$CoA such that a final concentration of 300 μM $C_4$CoA per well was achieved. Detection of the oxidation of NADH to $NAD^+$ was followed at $\varepsilon = 340$ nm using Constar 96-well plates. A typical inhibitor concentration range of 10 mM to 10 nM was utilized in an $IC_{50}$ determination where fitted curves were determined using KaleidaGraph Version 35.